Available online at www.sciencedirect.com

ScienceDirect

Energy Procedia 149 (2018) 435–444

Energy Procedia

www.elsevier.com/locate/procedia

16th International Symposium on District Heating and Cooling, DHC2018, 9–12 September 2018, Hamburg, Germany

Numerical Investigations on District Heating Pipelines Under Combined Axial And Lateral Loading

Tim Gerlach*[1], Martin Achmus[1], Mauricio Terceros[1]

[1]*Institute for Geotechnical Engineering, Leibniz University Hannover, Appelstr. 9A, 30167 Hanover, Germany*

Abstract

Within the design process of district heating networks, the soil resistances in axial and lateral pipeline direction are commonly treated independently as friction resistance and bedding pressure. However, at curved segments or near ellbows, these resistances occur simultaneously and affect each other. The state of knowledge regarding this topic is summarized, and it is shown that only limited information exists for this case of loading.

Therefore, a three-dimensional finite element model was developed, using the sophisticated concept of hypoplasticity as an advanced constitutive model for the bedding material. This soil model is able to account for dilatancy, barotropy and pycnotropy of granular soils. Subsequently, variations of the loading direction were performed for a reference system. The investigations give a good insight into the behaviour of district heating pipelines under combined loading, showing the interdependency of skin friction resistance and bedding pressure. We present a design approach which incorporates interaction terms, derived from the presented investigations. Results gained from these investigation are then transferred to the academic district heating network design tool IGtH-Heat, to evaluate in which manner the incorporation of coupling terms between bedding and friction resistance influences the pipe-soil interaction. Additionally, a temperature dependent formulation of maximum friction resistance is adopted to incorporate the effects of radial pipe displacement. Thereby we demonstrate that the predicted pipeline's displacement significantly change when these effects are taken into account. Using this new formulation, model predictions are compared to data from full scale field measurements.

* Corresponding author. Tel.: +49-511-762-3529; fax: 49-511-762-5105.
E-mail address: gerlach@igth.uni-hannover.de

1876-6102
10.1016/j.egypro.2018.08.208

Keywords: *Soil-structure interaction; numerical modelling; buried pipelines; combined loading*

1. Introduction

Nowadays, an efficient handling of resources is of special importance for our society. In consequence, the energy from former unused industrial waste heat gets increasingly utilized. Through combined heat and power, the heat waste gets transported by district heating networks to public buildings or private households. For transportation, preinsulated pipelines are predominantly used. They consist of three components that serve different purposes: the steel medium pipe transports the hot water and bears the primary portion of the load, while the outer layer (HDPE) protects the insulation material from water, harmful solids, and mechanical influences. The primary function of the polyurethane rigid foam is the insulation of the pipeline. As a side-effect, it also transfers loads between the medium and the casing pipe. Traditionally, a feed and a return line are installed at the same depth. The pipeline and the filling zone are usually filled with sand, that gets compacted in several layers.

During the operation of district heating networks, changes of the media temperature lead to periodic varying loading conditions. Hereby, the free movement of the pipe, which tends to elongate and shorten under temperature load, is hindered by the adjacent soil. The resistance of the soil can be divided into axial friction resistance and lateral bedding resistance. While both components have already been investigated independently of each other by several authors, the knowledge concerning interaction effects is limited. However, it is evident from figure 1, that near curves or elbow segments both bedding and friction resistances get mobilized and may affect each other.

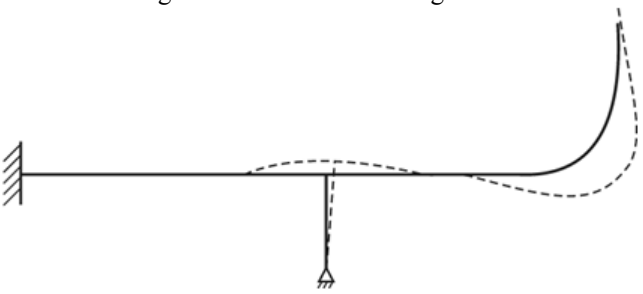

Figure 1: Displacement of temperature loaded, buried district heating system [1]

2. State of the art

2.1. Axial friction resistance

In common design practice in Germany [2], the maximum friction resistance is estimated from:

$$F_{R,u} = \mu \cdot \left(F_N' + F_G'\right). \tag{1}$$

Herein $F_{R,u}$ denotes the maximum resistance force per meter length, μ is the friction coefficient and F_N' and F_G' are the integrated normal stresses around the pipes circumference and the sum weight force of the filled pipeline, respectively. To incorporate the effects resulting from changes of operating temperature, the coefficient of contact friction is taken to $\mu = 0.4$ for increasing temperature conditions. During unloading (decrease of temperature), a value of $\mu = 0.2$ shall be applied [2]. However, the coefficient of contact friction is a material specific constant.

In general, the estimation of the maximum resistance force is based on Coulomb's friction law [3]. Following *Coulomb*, the maximum shear stress that can be mobilized between the pipe's mantle and the surrounding soil is proportional to the current normal stress. The constant of proportionality is the coefficient of contact friction μ. Neglecting the shear stresses in circumferential direction, the maximum resistance force that soil can exert on the pipeline due to axial relative displacement can be calculated from equation 1, wherein

$$F_N' = \sigma_0 * \pi * D_a * \frac{1+k_0}{2}. \quad (2)$$

Herein D_a denotes the outer diameter of the pipeline and k_0 is the coefficient of earth pressure at rest. Assuming the groundwater level to be beneath the bottom of the pipeline, the overburden stress at the centre of the pipeline is considered as the average normal stress σ_0:

$$\sigma_0 = \gamma * H. \quad (3)$$

The coefficient of earth pressure at rest can be estimated by the use of *Jaky*'s formula [4]:

$$k_0 = 1 - \sin(\varphi'). \quad (4)$$

Gramm [5] recommended an increased coefficient of earth pressure at rest, resulting from the densification process during the installation of the pipeline. Values between $0.5 < k_0 < 0.85$ are proposed, dependent on the intensity of densification.

The second term in brackets of equation 1 denotes the sum weight force of the pipeline:

$$F_G' = 2 * \pi * r_m * s * \gamma_s + \pi * r_i^2 * \gamma_w, \quad (5)$$

where r_m and r_i are the mean and the inner radius of the medium pipe, respectively. The wall thickness is denoted with s and γ_s and γ_w are the steel and water unit weights.

2.2. Radial pipe expansion

A change of media temperature leads to thermal strains within the pipeline. They evolve in both axial and radial pipe direction, while for the design, solely the axial strains are directly considered. As mentioned before, effects from radial expansion are only accounted for by using different coefficients of contact friction. Actually, the coefficient of contact friction is a constant and the increased friction, observed for pipelines subjected to a rise of temperature, results from higher contact normal stresses.

An increase of friction resistance was experimentally observed by several authors. Within full scale field tests by *HEW* (1987) [6], two DN700 pipelines of 19.65m length were installed and tested under different thermal conditions. Overburden heights of 0.8m and 1.15m were realized. Within 57 tests a dependency on medium temperature as well as on ambient temperature was observed. The maximum friction force at T=136°C medium temperature was about four times greater compared to T=18°C. Further experimental investigations were made by *Gietzelt et al.* (1991) [7]. Pipelines of different diameter were tested in a 25m long trench with concrete walls. For an increase of temperature of ΔT=100K a two times greater resistance force was measured. *Huber and Wijewickreme* (2014) [8] presented results from experimental tests using a pipeline with an outer diameter of D=520mm. Inside a chamber 3.8m*2.5m*2.5m, pipelines with different medium temperatures were axially displaced until failure. For ΔT=50K an increase of maximum resistance force could be observed. An about 10% higher value was measured, which is only a small increase compared to the aforementioned investigations.

Within the investigations on radial pipeline extension by *Achmus* (1995) [9], first the ratio between changes of media temperature to mantle temperature was evaluated. Assuming rotational symmetry of heat flux, the mantle temperature was calculated using the method of fictive heat sources and sinks. In a next step, the radial displacement was evaluated. For the steel pipe and the mantle, the theory of thin-walled shells and for the insulation the shell theory in plain strain conditions was considered. The same methodology was also used by *Beilke* (1993) [10].

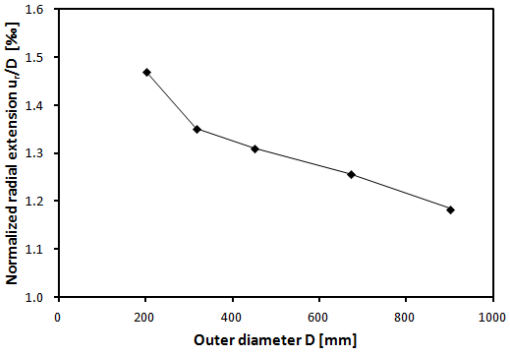

Figure 2: Normalized radial extension dependent on diameter for ΔT=120K [9].

For an increase of medium temperature ΔT=120K, the radial displacements normalized on diameter are depicted in Figure 2 for different pipeline diameters. Due to the high stiffness of the steel pipe compared to the other materials involved, changes of inner pressure and initial soil stress state were found to have only minor influence on the radial expansion.

Based on this work, an improved numerical model was presented by *Gerlach & Achmus* (2016) [11] using the sophisticated HSsmall model to describe the complex stress-strain behavior of the bedding material. The HSsmall accounts for an increased stiffness of soil in the small strain region, which leads to slightly higher increase factors κ. Based on comprehensive parametric studies, a corrective term was established to describe the changes of maximum friction force for arbitrary geometric conditions and soil properties. Due to the incorporation of small strain stiffness, the relation between media temperature and increase of resistance was found to be nonlinear.

2.3. Bedding resistance

The second main reaction component of the subsoil is the lateral resistance force $F_{B,}$ or the average bedding pressure $p_{m,}$ dependent on the lateral deflection y.

The first publication on this subject was presented by *Audibert & Nyman* (1977). They carried out a laboratory test series where the influence of soil density, pipe diameter and embedment ratio was investigated. A detailed description of the test setup can be found in [12]. The scope of laboratory investigations included three different diameters, the distinction between loose and dense sand and the variation of cover ratio. Additionally, one field test was carried out. As a schematic result, *Audibert & Nyman* pointed out two kinds of failure mechanisms dependent on the embedment depth. This was possible due to a transparent plexiglas window, which made the inspection of the soil movement possible. It was found that for shallow burials, less than three times of the pipe's diameter, two wedges are formed. A passive wedge can by observed in front of the pipe (in direction of displacement). Behind the pipe, a smaller, nearly vertical wedge is forming an active zone. With increasing burial depth, the lower bounds of the wedges become steeper and a separating zone forms between the two wedges, in which no vertical movement of the soil is observed.

Another goal was to find an analytical representation for the soil resistance-displacement relationship. A nonlinear curve which represents the relation of bedding resistance p over displacement y from the initial state to the maximal displacement y_u was found. At y_u, the soil reaction force reaches its maximum value p_u. According to *Audibert & Nyman*, the normalized bedding resistance $\tilde{p}$ over the normalized displacement $\tilde{y}$ can be approximated by:

$$\tilde{p} = \frac{\tilde{y}}{A_{lat} + (1 - A_{lat}) \cdot \tilde{y}}. \tag{6}$$

A_{lat} denotes the form factor that defines the initial stiffness and was found to be in the range of $0.145 - 0.2$. The two normalized parameters are defined as:

$$\widetilde{p} = \frac{p}{p_u} \qquad \text{and} \qquad \widetilde{y} = \frac{y}{y_u} . \tag{7}$$

So, to predict the bedding resistance for any state of displacement the maximum bedding resistance p_u and the maximum displacement y_u are needed. The maximum of bedding resistance can be obtained from:

$$p_u = \gamma \cdot H \cdot N_u . \tag{8}$$

Herein, N_u is a bearing capacity factor found by *Brinch Hansen* (1961) [13]. This factor can be taken from a chart, depending on the angle of internal friction and the cover ratio. *Audibert & Nyman* found a good agreement between their experimental laboratory and field tests carried out by *Brinch Hansen*.

Many design recommendations refer to their work, e.g. the most comprehensive code for district heating networks by *AGFW* [2]. Distinction is made between dense and loose sand. For loose sand holds:

$$N_u = \left[-12.34138 \cdot e^{-0.07628616 \cdot \frac{H}{D_a}} + 17.31058 \right], \tag{9}$$

$$y_u = 0.020 \cdot (h + D_a) . \tag{10}$$

Further experimental work was carried out by *Trautmann & O′ Rourke* (1985) [14]. A total of 30 lateral loading tests were performed. The relation between normalized bedding resistance $\tilde{p}$ over normalized displacement $\tilde{y}$ was found similar to *Audibert & Nyman*, while the bearing capacity factors are much lower.

This could be identified by *Achmus* [9] as an effect of diameter. Within his finite element modelling in plane strain conditions, the influences of cover ratio, distance to the border of the trench, and pipe diameter were investigated. It is pointed out that the diameter of the pipe obeys a functional relation of the bearing capacity factor. This gives an explanation for the differing values of the bearing capacity factor as determined by *Audibert &Nyman*, who mainly investigated pipes with diameters of $D = 25mm$ and $D = 60mm$, and *Trautmann & O′ Rourke*, who used pipes with $D = 102mm$ and $D = 324mm$.

2.4. Interaction

In the previous subsections we presented the descriptions of resistance components, holding if both of them are treated independently. Briefly, if solely pure axial or pure lateral pipe displacements are considered. As depicted in figure 1, this assumption does not match the real displacement paths of several pipeline segments, especially at and near curved sections. Here, the displacement is a combination of both local directions and thus, the occurring bedding and friction resistances may affect each other.

This interaction was investigated experimentally and numerically by a few authors. Thereby, the simplification was made that only a bidirectional movement of a rigid pipeline was taken into account and a possible rotation or bending was neglected. The angle of attack θ defines the angle between the pipelines displacement vector norm and the axial direction, e.g. $\theta = 0°$ describes pure axial movement. *Hsu et al.* (2001, 2006) presented results from experimental investigations in loose [15] and dense [16] sand. Within their scope of work, pipelines with different diameters were subjected to oblique displacement in a testing box. Regardless of deposit density, diameter and embedment ratio, it was found that the maximum bedding resistance is lowered by a simultaneous occurrence of axial displacement, while the maximum friction resistance is increased by the bedding reaction in lateral direction.

Further investigations were carried out by *Daiyan et al*. (2011) [17], who considered a small scale model in combination with a centrifuge and finite element modeling. They found the maximum bedding resistance to be up to 30% reduced in comparison with pure lateral loading. A more significant influence was observed for the axial component: For an oblique angle of $\theta \approx 40°$, the friction resistance was about 2.5 times higher compared to pure axial displacement. In addition, a two part failure mechanism was proposed. While for small oblique angles the failure occurs in circumference of the pipeline, with greater angles it turns into bearing failure through the subsoil.

3. Numerical modeling

3.1. Model

The presented investigations give a first insight into the impact of interaction effects due to bidirectional loading. However, for the development of an approach of practical usability, more comprehensive studies are necessary. Therefore, a three dimensional finite element model using the commercial software package ABAQUS [18] was established. The reference model consists of a rigid pipeline with an outer diameter of $D = 0.25m$ (DN150), the overburden height is $h = 0.8m$. The adjacent soil is assumed to be a homogenous loose sand ($D_r = 0.4$), so that no layering or influences of the trench walls are considered. For the soil domain, continuum elements with linear shape functions come into use. Within the soil layer a size bias is used so that the size of the elements is increasing with the distance from the pipe. Hence, the region near the pipe can be discretized finer than the elements at a larger distance where the mesh density can usually be reduced because of lower stress gradients. The resulting finite element model is depicted in figure 3.

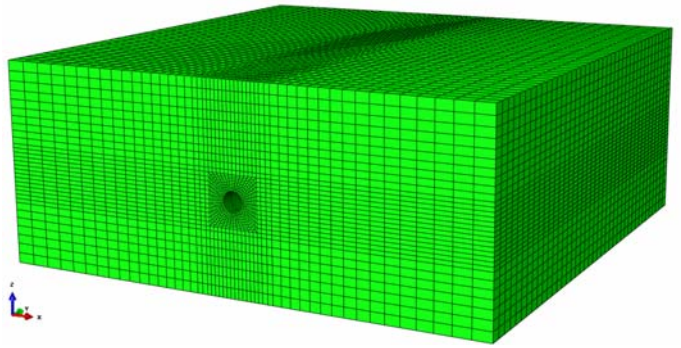

Figure 3: Finite element mesh used for the calculations

The constitutive law of hypoplasticity is used to describe the soil stress-strain behaviour. An implementation of hypoplasticity as an ABAQUS compatible user material (umat) is employed [19]. The hypoplastic material law is a rate-type model which accounts for the complex non-linear soil behaviour by just one (rather sophisticated) tensorial equation. In its form by *von Wolffersdorff*, the hypoplastic material law needs eight parameters [20]. It uses the stress state and the void ratio of a non-cohesive material as state variables and accounts for stress-dependence of soil stiffness and soil strength, thereby reflecting contractancy or dilatancy of soils under shearing in a realistic manner. For further description of the hypoplastic material model [20] is recommended while the considered set of material constants can be found in [21]. For a mean effective stress of $\sigma_m = 20kPa$, the angle of internal friction is $\varphi' \approx 35°$.

A relative displacement between the pipe and the surrounding soil occurs under oblique pipe movement. To enable the possibility of relative slipping within the finite element model, a contact condition is defined. The frictional contact is established using the simple friction law according to Coulomb. Following the guideline recommendations, the coefficient of contact friction is set to $\mu = 0.4$.

The calculation consists of three phases. In the first phase solely the soil domain is present in order to establish the geostatic stress state. In the following step, the pipeline as well as the contact condition are activated. During the final phase, the pipeline gets displaced with a predefined oblique angle by a reference node. The resulting contact

forces are extracted only from the middle third of the model to exclude possible boundary effects from the solution.

3.2. Results

Within a parametric study, 13 different oblique angles were considered. The results gained from the finite element model are depicted in figure 4 (grey lines) in terms of force-displacement curves. The left diagram shows the evolution of friction force over axial pipeline displacement. It is obvious that the coincident occurrence of both resistance components has a significant influence on the axial friction resistance. Due to the mobilization of bedding pressures, the average normal stress acting on the pipeline gets increased. This increased average normal stress, multiplied with the coefficient of friction, results in higher friction forces compared to the case of pure axial displacement. For small oblique angles, the increase of friction resistance is almost linearly related to the increase of bedding pressure. If the oblique angle becomes larger, the failure mechanism changes, as also observed by *Daiyan et al.*, and the shear failure through the subsoil leads to a complex state of stress and soil disturbance. Then, the formulation of interdependency between bedding and friction resistance becomes more complex. This can be explained by the fact that, besides the (horizontal) bedding pressure, also the vertical stress state in the pipelines circumference changes and affect the average normal stress.

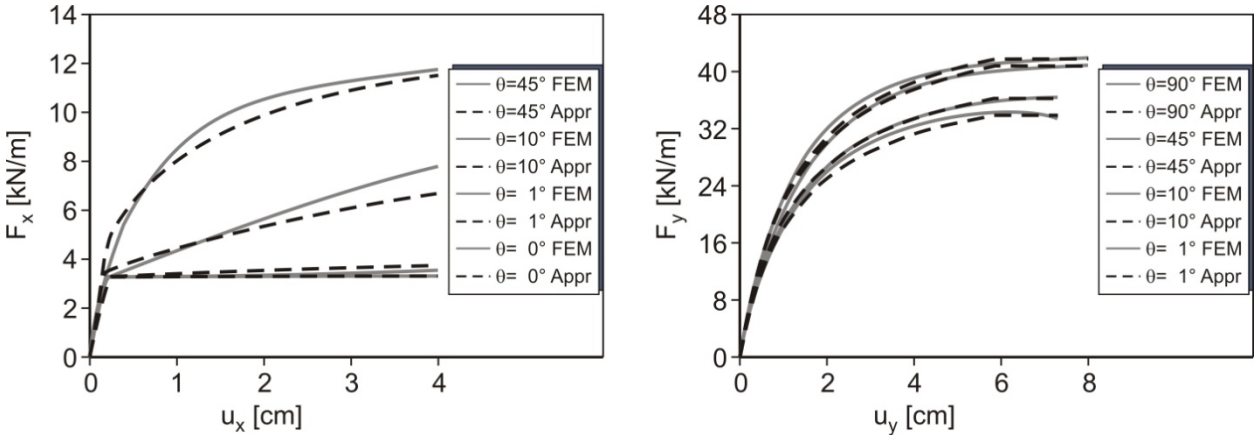

Figure 4: Force-displacement curves for different oblique angles

In contrast to the friction resistance, the impact of interaction on the bedding pressure is less pronounced. Figure 4 (right) shows the relation of bedding reaction force over lateral pipeline displacement. For small oblique angles, a reduction of maximum bedding force of about 20% can be observed. However, to reach these magnitudes of lateral displacement under small oblique angles, axial displacements are needed that are far beyond practical order. Nevertheless, the effects on bedding pressure are also considered in the following derivation of an improved description of spring stiffnesses.

3.3. Design approach

To incorporate the effects of interaction and radial pipeline expansion to the formulation of bedding and friction stiffness, we firstly refer to the procedure of *Audibert & Nyman* to describe the evolution of bedding resistance (cf. equations 6-10). Additionally, we take the oblique angle dependent reduction of maximum bedding force into account:

$$F_{B,u}(\theta) = \chi(\theta) \cdot (\gamma \cdot H \cdot N_u \cdot D), \tag{11}$$

with:

$$\chi(\theta) = \min((0.006 \cdot \theta + 0.807), (-0.0000108 \cdot \theta^2 + 0.00199 \cdot \theta + 0.907)), \quad (12)$$

Herein, χ is was calibrated against the results from the numerical model and reflects also the transition between the two failure mechanisms. As depicted in figure 5, a good agreement between the numerical results and the predicted maximum bedding force could be achieved.

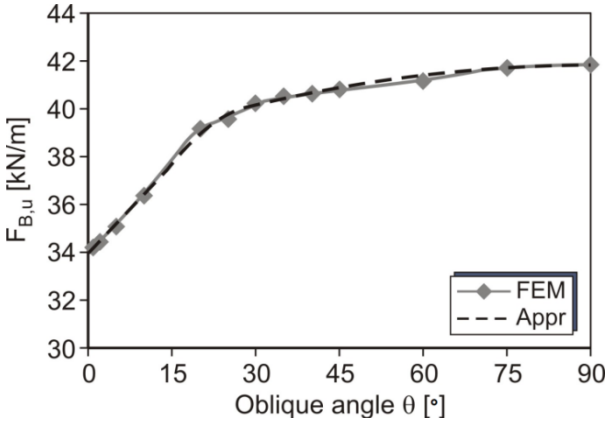

Figure 5: Maximum bedding force in dependency of oblique angle

The formulation of frictional spring stiffness needs to account for both interaction effects and radial pipe expansion. Therefore, we substitute F_N', the integrated normal stresses around the pipes circumference, by its oblique angle and media temperature dependent counterpart. Equation 1 can then be rewritten:

$$F_{R,u} = \mu \cdot \left(F_N'(\theta, T) + F_G'\right). \quad (13)$$

The substituted term can be decomposed in two parts:

$$F_N'(\theta, T) = \zeta \cdot F_B(\theta) + \kappa_T(T) \cdot F_N'. \quad (14)$$

To account for interaction effects, ζ denotes the amount of actual, oblique angle dependent bedding force F_B, that increases the average radial stress state. For the reference system, a value of $\zeta = 0.55$ was found to be an good agreement with the finite element results (cf. figure 4). F_N' in the second term refers to unmodified equation 2, multiplied with κ_T, denoting the ratio of initial average radial stress to the average radial stress dependent on the actual temperature :

$$\kappa_T(T) = \frac{\Delta\sigma_r(T)}{\sigma_0} + 1. \quad (15)$$

For the derivation of the change of radial stress $\Delta\sigma_r(T)$, we adopt the elastic solution of a plate with hole:

$$\Delta\sigma_r(T) = \frac{E'(\sigma_0)}{1+\nu} \cdot \frac{\Delta r(T)}{0.5 \cdot D_a}. \quad (16)$$

Herein, ν is the Poisson's ratio and $E'(\sigma_0)$ the stress dependent Young's modulus:

$$E'(\sigma_0) = \kappa \cdot 100kPa \cdot \left(\frac{\sigma_0}{100kPa} \right)^{\lambda} \cdot \frac{(1+\nu)\cdot(1-2\cdot\nu)}{1-\nu}. \quad (17)$$

κ and λ are material dependent constants to account for stress dependent stiffness of soil and can be determined by oedometric tests. Finally, the change of pipeline diameter (here: radius) can be estimated from the temperature increment and mantle displacement for a temperature rise of $T = 120K$, as proposed by *Achmus* (cf. figure 2):

$$\Delta r(T) = \frac{T_i - T_{i-1}}{120K} \cdot u_{r,\Delta T=120K}. \quad (18)$$

For simplification, we assume that the interaction independent part of friction resistance increases linearly up to $x_u = 0.01D$.

4. Holistic simulation using IGtH-Heat

The presented design approach was implemented into the academic district heating network design tool IGtH-Heat, which adopts the temperature-loaded pipeline as beams according to Bernoulli's theory and the soil reaction as nonlinear springs. Due to this nonlinearity, Newton-Raphson method is used to solve the set of equations. For validation, data from a full scale field testing network were provided by our research partner *AGFW*. The test site is located in Chemnitz (Germany) and consists of four geometrically identical pipeline systems. Its geometry is depicted in figure 6.

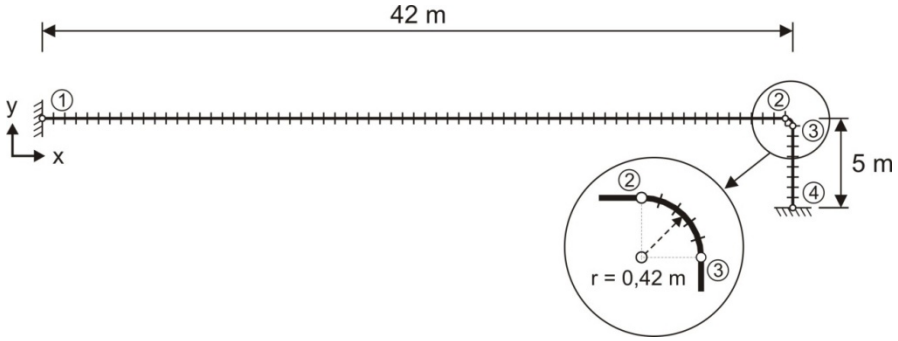

Figure 6: Geometry of the testing pipeline in Chemnitz (Germany)

The pipeline is a DN150 ($D = 0{,}15m$) embedded in medium-fine sand ($d_{10} = 0.08m$; $U = 2.4$; $D_r = 0.4$). The overburden height is $h = 0.8m$. Geotechnical investigations were carried out in field and laboratory and resulted in a coefficient of earth pressure of $k_0 = 0.5$, a soil unit weight of $\gamma' = 15.2kN/m^3$, stress dependent constants of $\kappa = 210$ and $\lambda = 0.5$ as well as an a peak friction angle of $\varphi' = 35.5°$. The coefficient of contact friction was evaluated by direct shear tests to be $\mu = 0.415$. The remaining inputs are based on (2).

To compare the IGtH-Heat prediction with field data, the initial heating phase is considered. Therein, the media temperature rises from $T = 13.2°C$ to $T = 88.0°C$. In consequence, the same loading was adopted for the design calculation. The axial displacements are compared at $x = 40m$. In the test side, an axial movement of $u = 23.5mm$ was measured. In IGtH-Heat, firstly a calculation was carried out under neglection of interaction effects or influences from radial expansion. Thereby, a displacement of $u = 26.6mm$ resulted, which is a deviation of approximately 13%. Subsequently, the media temperature dependent formulation of frictional spring stiffness was taken into account, leading to a calculated displacement of $u = 25.4mm$, which represents a deviation of 8%. In the final validation step, interaction effects were accounted for in addition. The resulting displacement was $u = 24.8mm$ or in terms of deviation: 5.5%. Thus, the deviation could be more than halved based on the proposed design approach for lateral and axial spring stiffness.

4. Conclusion and perspective

Within the paper at hand, the interaction of the soils reaction components bedding pressure and friction resistance was investigated. Therefore, after a brief introduction, the state of knowledge was summarized. In the following, a three dimensional finite element was introduced, using the sophisticated hypoplastic material model to describe the stress-strain behavior of the soil. For a reference system, the oblique angle was varied in a wide range. Based on these results, new formulations for both reaction components were proposed. In addition, the temperature dependent radial pipeline extension and the resulting stress changes within the soil were incorporated.

Finally, these design approaches were implemented into the academic design code IGtH-Heat. Therewith, calculations were carried out in order to compare them to field data. It was shown, that by the use of the new formulations, the deviation between prediction and measurement could be more than halved (13% -> 5.5%).

In future work we intend to extend the numerical modeling to different geometric properties in terms of diameter and embedment depth as well as a variation of soils deposit density.

Acknowledgements

The presented research work was funded by the German Federal Ministry of Economic Affairs and Energy under Grant number 03ET1335B. The support is gratefully acknowledged.

References

[1] Achmus, Martin and Weidlich, Ingo. "Interaktion zwischen Fernwärmeleitungen und dem umgebenden Boden". *Bautechnik 93 (*2016), 663-671. (in German)
[2] AGFW e.V. "Verlegung und Statik von Kunststoffmantelrohren (KMR) für Fernwärmenetze" (2007). (in German)
[3] Coulomb, C. A. "Essai sur une application des regles des maximis et minimis a quelquels problems de statique relatifs, a la architecture". *Mem. Acad. Roy. Div.Sav*. 7. 1776, 343–387 . (in French)
[4] Jaky, J. "Pressure in silos", London (1948), Vol. 1, 2nd ICSMFE. 1948, 103-107.
[5] Gramm, G. "Statik und Festigkeit des Kunststoffmantelrohres". *3R International* Jg. 22, Nr.7/8. (1983), 355–357. (in German)
[6] HEW. "Fernwärmetransportleitung Karoline-Wedel Kunststoffmantelrohr DN 700". Hannover, (1987). (in German)
[7] Gietzelt, M., et al. "Ermittlung der Reibungskräfte an erdverlegten wärmeführenden Leitungen zur Sicherstellung wirtschaftlicher Konstruktionen". (1991). (in German)
[8] Huber, M. and Wijewickreme, D. "Thermal Influence on Axial Pullout Resistance of Buried District Heating Pipes". Stockholm, Sweden, (2014). *14th International Symposium on District Heating and Cooling*.
[9] Achmus, Martin. "Zur Berechnung der Beanspruchungen und Verschiebungen erdverlegter Fernwärmeleitungen". Hannover: Institut für Grundbau, Bodenmechanik und Energiewasserbau, (1995). (in German)
[10] Beilke, O. Interaktionsverhalten des Bauwerks “Fernwärmeleitung-Bettungsmaterial". Institut für Grundbau, Bodenmechanik und Energiewasserbau, (1993). (in German)
[11] Gerlach, Tim and Achmus, Martin. "On the influence of thermally induced radial pipe extension on the axial friction resistance". *Energy Procedia*. (2017), Vol. 116, pp. 351-364.
[12] Audibert, Jean ME and Nyman, Kenneth J. "Soil restraint against horizontal motion of pipes". *Journal of the Geotechnical Engineering Division*. (1977), Vol. 103, pp. 1119-1142.
[13] Hansen, J.B.. and Christensen, N.H. "The Ultimate Resistance of Rigid Piles Against Transversal Forces: Model Tests with Tranversally Loaded Rigid Piles in Sand". Geoteknisk Institut (1961).
[14] Trautmann, Charles H. and O’Rourke, Thomas D. "Lateral force-displacement response of buried pipe". *Journal of Geotechnical Engineering*. 9 (1985) Vol. 111, pp. 1077–1092.
[15] Hsu, T. W., Chen, Y. J., & Wu, C. Y. "Soil friction restraint of oblique pipelines in loose sand". *Journal of transportation engineering*. (2001), Vol. 127(1), pp. 82-87.
[16] Hsu, T. W., Chen, Y. J., & Hung, W. C. "Soil restraint to oblique movement of buried pipes in dense sand". Journal *of Transportation Engineering*. (2006), Vol. 132(2), pp. 175-181.
[17] Daiyan, N., Kenny, S., Phillips, R., & Popescu, R. "Investigating pipeline–soil interaction under axial–lateral relative movements in sand". *Canadian Geotechnical Journal*. (2011), Vol. 48(11), pp. 1683-1695.
[18] Hibbitt, D., Karlsson, B., & Sorensen, P. "ABAQUS 6.11: a computer software for finite element analysis" Dassault Systems, (2011)
[19] G. Gudehus, A. Amorosi, A. Gens, I. Herle, D. Kolymbas, D. Mašín, D. Muir Wood, R. Nova, A. Niemunis, M. Pastor, C. Tamagnini, and G. Viggiani. "The soilmodels.info project". *International Journal for Numerical and Analytical Methods in Geomechanics*. (2008), Vol. 12, 32, pp. 1571-1572.
[20] von Wolffersdorff, P. A. "A hypoplastic relation for granular materials with a predefined limit state surface". *Mechanics of Cohesive-frictional Materials*. (1996), Vol. 1(3), pp. 251-271.
[21] tom Wörden, Florian. "Untersuchungen zum räumlichen aktiven Erddruck auf starre vertikale Bauteile im nichtbindigen Boden": Institut für Grundbau, Bodenmechanik und Energiewasserbau (IGBE), (2010). (in German)